An Active Power Coordinated Control Strategy based on Droop Control for the Advanced Traction Power Supply System

Shuang Yang[1], Li Zeng[1], Hongmo Song[1], and Xiaoqiong He[1,2]
[1] School of Electrical Engineering, Southwest Jiaotong University, Chengdu, China
[2] National Rail Transit Electrification and Automation Engineering Technology Research Center, Southwest Jiaotong University, Chengdu, China

***Abstract*--The advanced traction power supply system (ATPSS) based on power electronic converter can eliminate the neutral sections, which can solve the drawbacks of the existing traction power supply system. Therefore, the ATPSS has attracted much attention. In order to realize the stability and efficiency of the system, proposed an active power coordinated control strategy based on droop control. The topology of the ATPSS is analyzed in this paper, the traditional droop control applied to the ATPSS can achieve equal power output from each substation, but when the locomotive is far from the substation, it will cause more losses on the traction network side. In order to achieve efficiency of the ATPSS, the substation is expected to adjust the output active power according to the position of the locomotive. Most secondary controls require known load conditions to achieve power coordination, but the constantly moving locomotives undoubtedly make communication more difficult. The strategy proposed in this paper can realize the power coordination control automatically without relying on vehicle-substation communication, to meet the required efficiency performance of the ATPSS. Finally, the proposed active power coordinated control strategy has been verified in simulation and experiment.**

***Index Terms*—ATPSS, droop control, active power coordination.**

I. INTRODUCTION

Nowadays, most countries currently use three-phase to two-phase traction transformer for traction power supply systems(TPSS), which have inherent drawbacks such as neutral sections and poor power quality, limiting the speed and capacity of railroads [1]. As shown in Fig.1, the traditional TPSS constructed for the V/v traction transformer , in which the main causes of drawbacks are as follows:

1) For each traction substation(TSS), traditional traction transformer adopt different wiring methods, its output two phases exist phase difference, which can not be directly connected. Therefore, TPSS need to be supplemented with neutral section for isolation, which caused the existence of the defect that there are no power area in TPSS.

2) Since TPSS is single-phase power supply system, the traditional method cannot realize the symmetrical transformation from three-phase grid to single-phase traction network. Furthermore, the locomotive has randomness and mobility, and different traction power supply arm cannot guarantee the same load power. Therefore it bring power quality pollution to the three-phase grid, especially the negative sequence component. Even for a balanced traction transformer such as wood bridge, it still brings power quality pollution due to the inconsistent traction power supply arm[2-3].

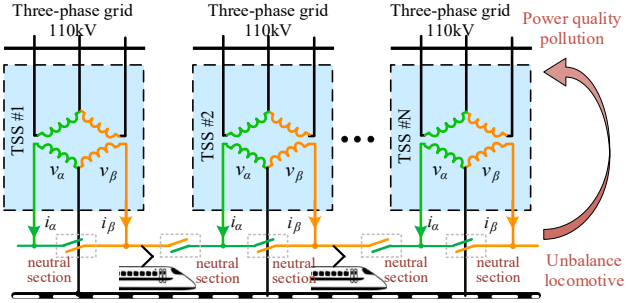

Fig. 1. Traditional TPSS constructed for V/v traction transformer

In order to address the drawbacks of the traditional TPSS, many improvements have been constructed to the TPSS worldwide, including the installation of a large number of compensation devices such as SVG, the adoption of automatic phase splitting technology, or direct improvement of the system, such as the Cophase traction power supply technology in China, which can improve the power quality while eliminating part of the electrical phase splitting of the system. It is reflected that the development of the system to realize through-phase power supply and solve the power quality problem is the future development trends [4].

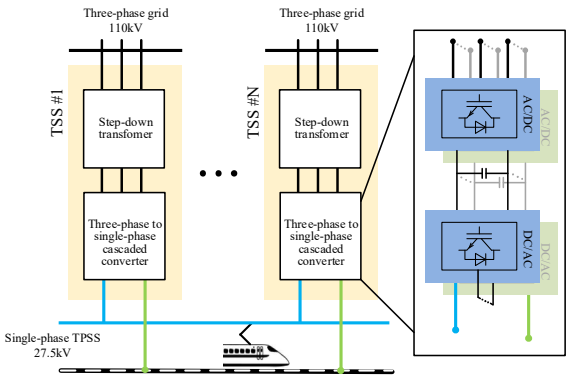

Fig. 2. ATPSS based on high power converters

Project supported by the National Natural Science Foundation of China (Grant No. 52077181)
Science and technology project of Henan Province (Grant No. 232102241041)

With the continuous development of power electronic technology, advanced traction power supply system (ATPSS) based on power electronic converters have emerged [5], as shown in Fig.2, which can solve the existing problems of traditional systems. ATPSS can achieve voltage controllable of traction network to achieve eliminate the neutral sections across the line. Meanwhile, the converter realizes three-phase to single-phase symmetrical transformation, solving the traction power supply system for grid generated by the negative sequence problem. Therefore, ATPSS has attracted much attention, and it is necessary to focus on grid-connected control technology of converters.

Reference [5] proposed a current-sharing control algorithm, but this strategy relies on a stable master substation output voltage, which make the system unreliable, if the collapse of the master may lead to system collapse; The grid-connected control technologies in reference [6] shows most secondary control needs load conditions available, for high-speed moving locomotive in ATPSS brings communication difficult, undoubtedly make harder to realize secondary control.

In this paper, proposed an active power coordinated control strategy based on droop control, which does not depend on the substation-locomotive communication and naturally realizes locomotives obtain more power from near substation, and verifies the correctness of the proposed strategy by Matlab/Simulink simulation and experiment.

II. The Topology of Advanced Traction Power Supply System

A. The Advanced Traction Power Supply System

Limit to the level of existing power electronic devices, the converter applied to the traction power supply at 27.5kV needs to be using a large number of high-power devices cascade and parallel [7]. As shown in Fig.3, single module is neutral point clamped (NPC) three-level inverter, then:

$$\begin{cases} \dfrac{U_{dc}}{\sqrt{2}} \cdot m \cdot n = U_S \\ U_s \cdot I_s \cdot x = C \end{cases} \tag{1}$$

where U_{dc} is the DC link voltage of single module, m is the modulation degree of cascaded inverter, n and x are respectively the number of cascaded module and parallel module, U_S and I_S are each cascaded module output root mean square (RMS) of voltage and current.

Obviously, U_S should meet the specification of TSS output, which in China is range of 24-31kV. U_{dc} and I_S are closely related to IGBT selection and substation capacity design. Then, the constraint condition is:

$$\begin{cases} 0 < m \le 1;\ 24000 \le U_S \le 31000; \\ U_C \le U_{dc} \le \dfrac{4}{3} U_C;\ \dfrac{3}{2} I_C \le I_S \le 2 I_C; \end{cases} \tag{2}$$

where U_C, I_C are voltage and current resistance of IGBT, generally consider 1.5-2 times margin. In this paper, selected parameters are: U_C/I_C = 4500V/3000A, C=40MVA. The values of each parameter are obtained as: n=9, x=1, U_{dc}=4800V.

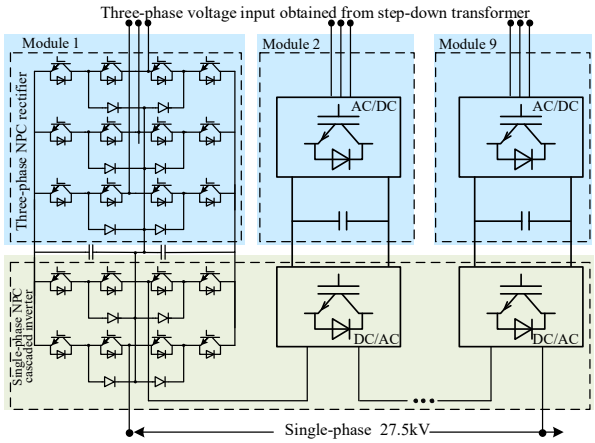

Fig. 3. ATPSS based on high power converters

B. Mathematical model and basic control of NPC converter

When there-phase rectifier is in stable operation, considering to be able to maintain DC stability, three-phase NPC rectifier and single-phase NPC inverter remain relatively independent.

For three-phase NPC rectifier, the mathematical model in a two-phase rotating coordinate system is established as:

$$\boldsymbol{u}_{dq} = \begin{bmatrix} \boldsymbol{u}_d \\ \boldsymbol{u}_q \end{bmatrix} = \begin{bmatrix} -L \cdot \dfrac{d\,\boldsymbol{i}_d}{d\,t} + \omega \cdot L \cdot \boldsymbol{i}_q - R\boldsymbol{i}_d + \sqrt{\dfrac{3}{2}} \cdot U_{max} \\ -L \cdot \dfrac{d\,\boldsymbol{i}_q}{d\,t} - \omega \cdot L \cdot \boldsymbol{i}_d - R\boldsymbol{i}_q \end{bmatrix} \tag{3}$$

where $\boldsymbol{u}_d$, $\boldsymbol{u}_q$ and $\boldsymbol{i}_d$, $\boldsymbol{i}_q$ are there-phase gird side voltage and current of dq-frame, L and R are there-phase grid side inductor and resistance, and assume L_a= L_b= L_c= L, R_a=R_b=R_c=R.

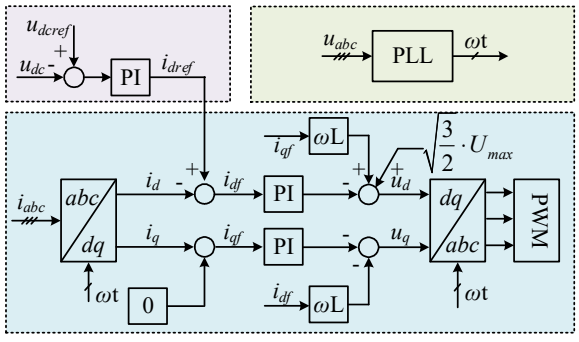

Fig. 4. Block diagram of three-phase NPC rectifier voltage and current double close-loop control

According to Equation (3), the three-phase NPC rectifier voltage and current double closed-loop control based on dq decoupled block diagram is obtained as Fig. 4.

For sing-phase cascaded inverter, which direct access to the traction, and it is impacted by locomotive. For security

reason, the same voltage and current double close-loop control based on *dq* decoupled.

To realize sing-phase *dq* decoupled double close-loop control, there is a need to construct virtual orthogonal quantity. In this paper, second order generalized integrator (SOGI) is adopted, obtained the $\boldsymbol{u}_{s\alpha}$, $\boldsymbol{u}_{s\beta}$, which are single-phase voltage of $\alpha\beta$ frame, then:

$$\begin{bmatrix} \boldsymbol{u}_{sd} \\ \boldsymbol{u}_{sq} \end{bmatrix} = C_{\alpha\beta\text{-}dq} \begin{bmatrix} \boldsymbol{u}_{s\alpha} \\ \boldsymbol{u}_{s\beta} \end{bmatrix} = \begin{bmatrix} \cos\theta & \sin\theta \\ -\sin\theta & \cos\theta \end{bmatrix} \begin{bmatrix} \boldsymbol{u}_{s\alpha} \\ \boldsymbol{u}_{s\beta} \end{bmatrix} \tag{4}$$

Meanwhile, the output current of single-phase cascaded inverter $\boldsymbol{i}_L$ also satisfies Equation (4). Assume to adopt *LC* filter, and $\boldsymbol{i}_s$ is the current after $\boldsymbol{i}_L$ passes through the *LC* filter, then the mathematical model in dq-frame of single-phase cascaded inverter is[8]:

$$\begin{cases} \boldsymbol{i}_{Ld} = \boldsymbol{i}_{sd} - \omega C_n \boldsymbol{u}_{sq} + C_n \dfrac{d\boldsymbol{u}_{sd}}{dt} \\ \boldsymbol{i}_{Lq} = \boldsymbol{i}_{sq} + \omega C_n \boldsymbol{u}_{sq} + C_n \dfrac{d\boldsymbol{u}_{sd}}{dt} \end{cases} \tag{5}$$

$$\begin{cases} \boldsymbol{u}_{sd} = \boldsymbol{u}_{Ld} + \omega L_n \boldsymbol{i}_{Lq} - L \dfrac{d\boldsymbol{i}_{Ld}}{dt} \\ \boldsymbol{u}_{sq} = \boldsymbol{u}_{Lq} - \omega L_n \boldsymbol{i}_{Ld} - L \dfrac{d\boldsymbol{i}_{Lq}}{dt} \end{cases} \tag{6}$$

where L_n, C_n are the inductor and capacitor of output *LC* filter.

According to Equation (5)-(6), the single-phase NPC cascaded inverter voltage and current double closed-loop control based on *dq* decoupled block diagram is obtained as Fig.5.

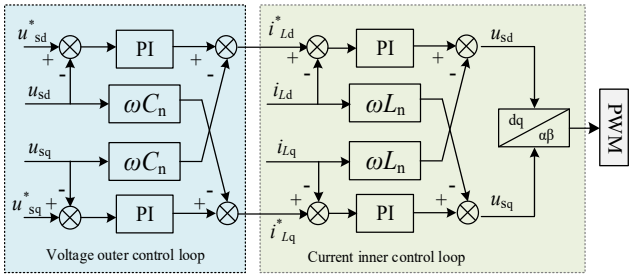

Fig. 5. Block diagram of single-phase NPC cascaded inverter voltage and current double close-loop control

III. An Active Power Coordinated Control Strategy based on Droop Control

A. Droop characteristic of the ATPSS

When ATPSS is operating, it can be equated to multiple distributed power sources operating in parallel. Then For each substation *i* (*i*=1, 2, 3…), its output power can be expressed as [6]:

$$P_i = \frac{(X_{si}+X_{ti})(V_{si}V_v\cos\delta_i - V_v^2) + (R_{si}+R_{ti})V_{si}V_v\sin\delta_i}{(X_{si}+X_{ti})^2 + (R_{si}+R_{ti})^2} \tag{7}$$

$$Q_i = \frac{(X_{si}+X_{ti})(V_{si}V_v\cos\delta_i - V_v^2) - (R_{si}+R_{ti})V_{si}V_v\sin\delta_i}{(X_{si}+X_{ti})^2 + (R_{si}+R_{ti})^2} \tag{8}$$

where P_i is the output active power of substation *i*; Q_i is the output reactive power of substation *i*; V_{si} is the output voltage amplitude of substation *i*; V_v is the port voltage of the locomotive; δ_i is the output voltage phase of substation *i*; R_{si} is the resistance of the substation *i*; R_{ti} is the resistance of traction network; X_{si} is the reactance of substation *i*; X_{ti} is the reactance of traction network.

Adopt uniform chain circuit model for traction networks, due to the traction network impedance is mainly inductive, the impedance angle of traction network is small enough to ignore the traction network resistance [9-10].

Approximately consider sin $\delta \approx\delta$, sin $\delta \approx 1$, and impedance of networks $X_{ti}>>X_{si}$, then:

$$P_i \approx \frac{V_{si}V_v\delta_i}{X_{ti}} \tag{9}$$

$$Q_i \approx \frac{V_v(V_{si}-V_v)}{X_{ti}} \tag{10}$$

B. Traditional droop control for the ATPSS

Droop control as a classical method of grid-forming control strategy, make the grid-connected converter in the form of voltage source. Each substation when droop control is adopted can participate in supporting the traction network voltage and frequency.

According to Equation (9)-(10), which shows the droop characteristic, then the droop control equation is:

$$\begin{cases} \omega_i = \omega_0 - k_n(P_i - P_{iref}) \\ V_{si} = V_{s0} - k_m(Q_i - Q_{iref}) \end{cases} \tag{11}$$

Equation (11) shows the traditional droop control strategy. As for active power, when locomotive is in different positions, caused different traction network reactance, i.e. $X_{t1}\neq X_{t2}$ (Assume locomotive is between first and second substations). At the same time, P_1 and P_2 are changing, frequency ω_1 and ω_2 are also changing, until reach the goal of $\omega_1=\omega_2$, e.i. $P_1=P_2$.

C. The proposed active power coordinated control strategy for the ATPSS

To realize active power coordinated control without substation-locomotive communication, proposed an active power coordinated control strategy as shown in Fig.6. By sending voltage signals u_{si} to the secondary control system , obtain the corner frequency adjustment signal ω_{pci} of each substation.

Then, active power droop characteristic shown as:

$$\omega_i = \omega_0 + \omega_{pci} - k_n(P_i - P_{iref}) \tag{12}$$

where ω is the angular velocity of substation; ω_0 is the rated angular velocity of substation; ω_{pci} is the frequency correction of secondary control; k_n is the active power

droop coefficient.

Corner frequency adjustment signal ω_{pci} realize the characteristic curves of the active power translation, as shown in Fig.7.

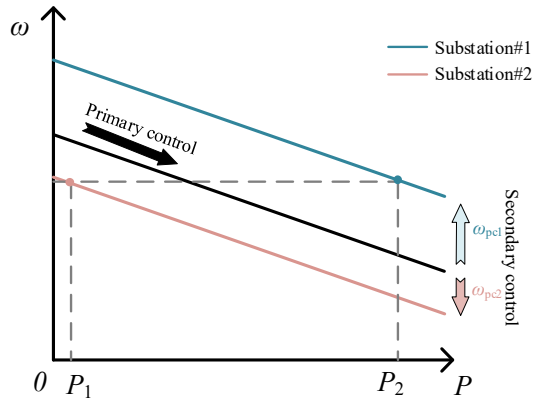

Fig. 7. The diagram of active power coordinated control strategy for the ATPSS

For the specific control strategy, the secondary control makes :

$$\delta_1 = \delta_2 = \cdots = \delta_n \tag{13}$$

Assume that the locomotive operates between substation 1 and 2, there is:

$$\frac{P_1}{P_2} = \frac{V_{s1}V_L\delta_1}{X_{t1}} / \frac{V_{s2}V_L\delta_2}{X_{t2}} = \frac{X_{t2}}{X_{t1}} \tag{14}$$

Considering the locomotive is constant power source, and the power is P_L, then:

$$P_1 = \frac{X_{t2}}{X_{t1}+X_{t2}}P_L;\ P_2 = \frac{X_{t1}}{X_{t1}+X_{t2}}P_L; \tag{15}$$

Combining the above Equation (12)-(15), then:

$$\omega_{pci} = k_n\left(\frac{X_t - X_{ti}}{X_t}\right)P_L - k_n P_{iref} \tag{16}$$

where X_t is the total reactance between the two substations, e.t. X_t=X_{ti} (Only if $X_{t(i+1)}$=0).

From above analyzing, compared to traditional droop control, obtain substation output active power as shown in Fig.6, active power coordinated control strategy proposed in this paper effectively realize active power optimization control, when locomotive is near a substation, it obtains more power from that substation accordingly, reducing traction network losses.

IV. Simulation and Experiment

A. Simulation Verification

The validity of the control strategy is verified through MATLAB/Simulink simulation. Parameters applied to the simulation are listed in Table I.

TABLE I

Parameter	Value
Molude number	9
Multi-winding step-down transformer	110kV/2.5kV
DC link voltage	4800V
DC link capacitance	5mF
Single-phase cascade output voltage	27.5kV
Single-phase output LC filter	5mH/50μF

For each module, the simulation result of there-phase NPC rectifier as shows in Fig.8 and Fig.9. The results

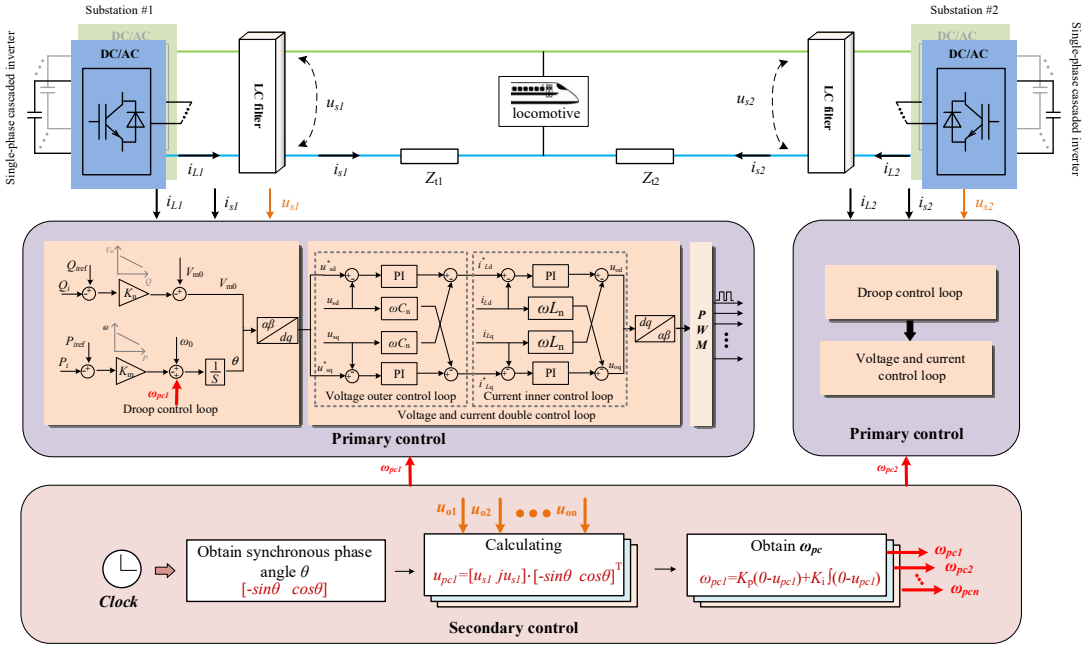

Fig. 6. The diagram of active power coordinated control strategy for the ATPSS

shows that the double closed-loop rectifier control based on *dq* decoupled achieves good power quality on the three-phase side and ensures stable DC voltage output.

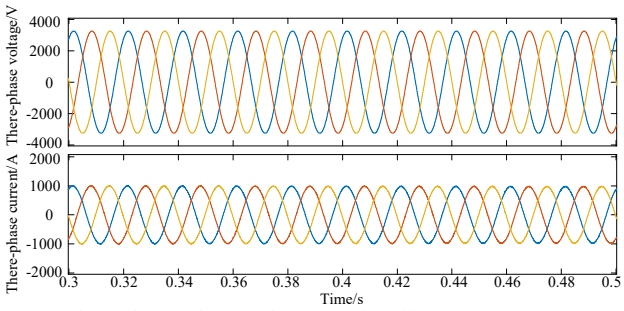

Fig. 8. There-phase voltage and current of rectifier

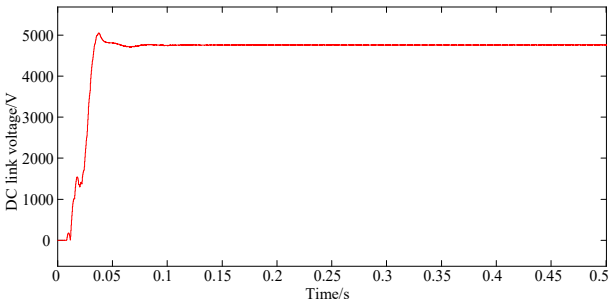

Fig. 9. DC link voltage

The simulation result of the single-phase cascaded inverter is shown in Figure 10, which ensures a stable output voltage of 27.5kV and good power quality.

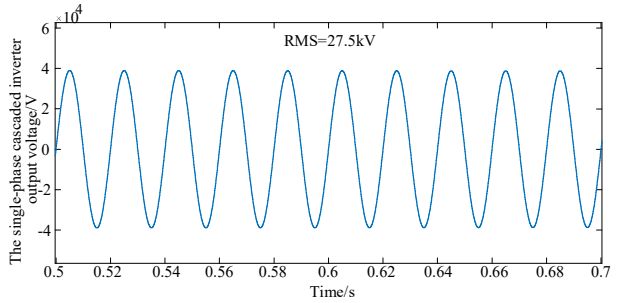

Fig. 10. Sing-phase voltage of cascaded inverter

The simulation results based on traditional droop control are shown in Fig. 11-12. Simulation of locomotive movement is carried out, and it can be seen that in the process of locomotive movement, phase adjustment exists in each substation to adjust its own output active power, finally achieve the output power basically consistent. and which is consistent with the theoretical analysis.

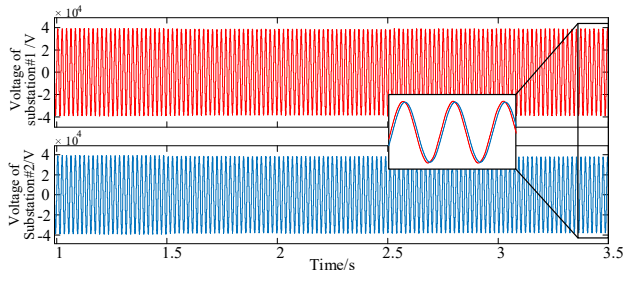

Fig. 11. Voltage of substation1,2 based on traditional droop control

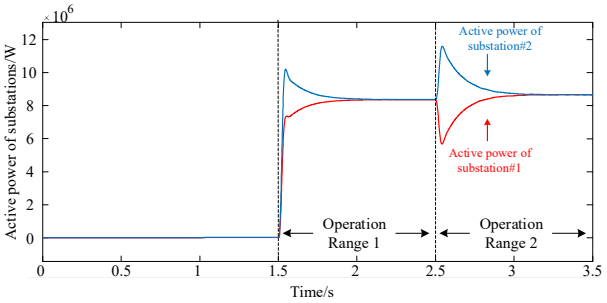

Fig. 12. Active power of substation1,2 based on traditional droop control

The simulation results based on proposed active power coordinated control strategy are shown in Fig.13-14. Four locomotive operation ranges are set up, and the output of each substation can be kept stable in locomotive moving all the time. Meanwhile, the proposed active power coordinated can realize the active power according to the distribution to reduce the line loss effectively. Verified the correctness of the proposed control strategy.

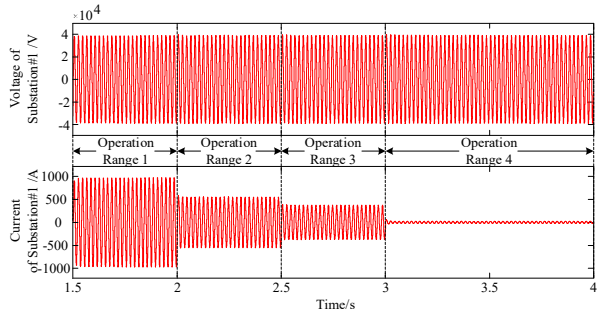

Fig. 13 Voltage and current of substation1 based on proposed active power coordinated control strategy

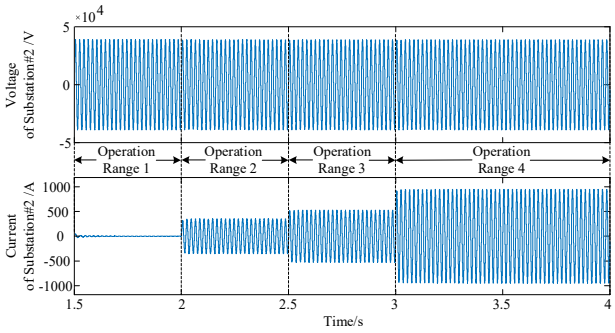

Fig. 14 Voltage and current of substation2 based on proposed active power coordinated control strategy

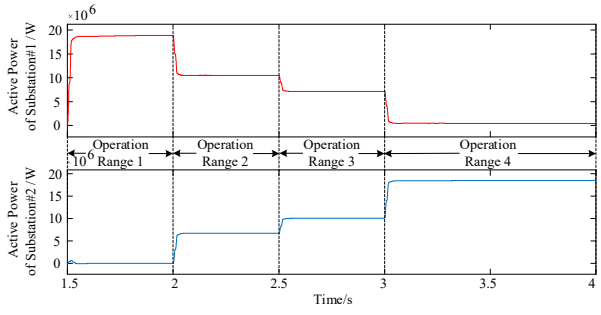

Fig. 15 Active power of substation1,2 based on proposed active power coordinated control strategy

B. Experiment Verification

The validity of the control strategy is verified through low power experimental platform, and parameters applied to the simulation are listed in Table II.

TABLE II

Parameter	Value
Three-phase phase voltage	50V
DC link voltage	100V
Sing-phase voltage	55V
DC link capacitance	470μF
Single-phase output LC filter	20μF/1mH

As shown in Fig.16, there-phase there-level NPC rectifier worked at steady state.

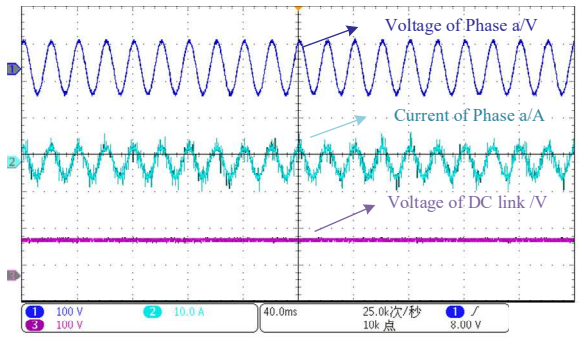

Fig. 16 Result of there-phase NPC rectifier

The experiment verification of grid-connected process, loading process and load moving process of two modules of converter was carried out, and the results were obtained as shown in Fig.17-18.

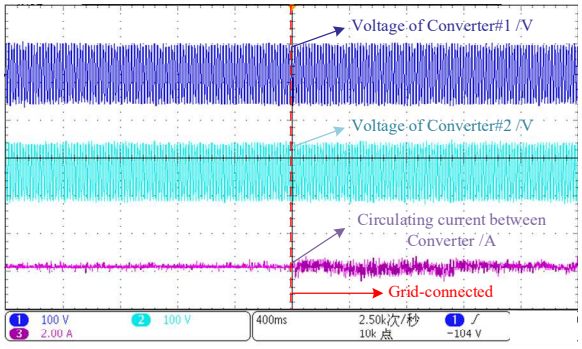

Fig. 17 Converter grid connection process

Fig.17 shows that the system is able to operate in parallel with a small circulating current.

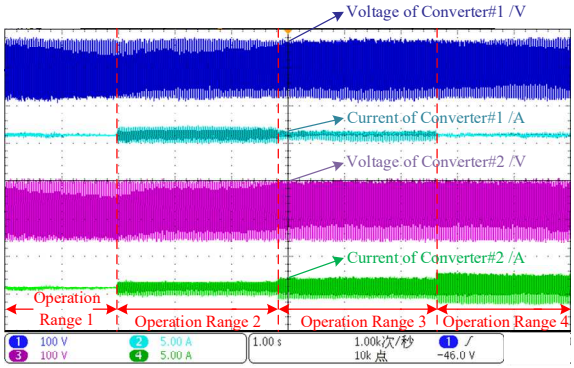

Fig. 18 Load moving process

Fig.18 shows that each converter can automatically change the output current and the output power according to the change of load position, which verifies the correctness of the proposed control strategy.

V. Conclusions

1. The ATPSS is investigated, and droop characteristic of ATPSS are analyzed based on uniform chain circuit model for traction networks.

2. In this paper, an active power coordinated control method for ATPSS is proposed, which realize substations stably grid connection. And when locomotive is going to a substation, it automatically obtains more power from that substation accordingly without substation-locomotive communication, reducing traction network losses.

3. Simulation and experiment results are given to validate the correctness of proposed active power coordinated control strategy.

References

[1] H. Hu, Z. He, X. Li, et al, "Power-Quality Impact Assessment for High-Speed Railway Associated With High-Speed Trains Using Train Timetable—Part I: Methodology and Modeling," *IEEE Transactions on Power Delivery*, vol. 31, no. 2, pp. 693-703.

[2] S. M. Gazafrudi, A. T. Langerudy, et al, "Power quality issues in railway electrification: A comprehensive perspective," *IEEE Transactions on Industrial Electronics*, vol. 62, no. 5, pp. 3081–3090, May 2015.

[3] P. Han, X. He, H. Ren, et al. Fault Diagnosis and System Reconfiguration Strategy of a Single-Phase Three-Level Neutral-Point-Clamped Cascaded Inverter [J] *IEEE Transactions on Industry Applications*. 2019, 55(4): 3863-3876.

[4] Z. Shu, S. X, K. L, et al., "Digital Detection, Control, and Distribution System for Co-Phase Traction Power Supply Application," *IEEE Transactions on Industrial Electronics*, vol. 60, no. 5, pp. 1831-1839.

[5] X. He, Z. Shu, et al, "Advanced Co-phase Traction Power Supply System Based on Three-Phase to Single-Phase Converter," *IEEE Transactions on Power Electronics*, vol. 29, no. 10, pp. 5323-5333, Oct. 2014.

[6] Y. Han, H. Li, et al, "Review of Active and Reactive Power Sharing Strategies in Hierarchical Controlled Microgrids," *IEEE Transactions on Power Electronics*, vol. 32, no. 3, pp. 2427-2451, March 2017.

[7] X.Q. He, P.C. Han, et al, "Study on Advanced Cophase Traction Power Substation System Based on Cascade-parallel Converter," *Journal of the China Railway Society*, vol. 39, no. 8, pp.52-61, 2017.

[8] M. A. Vitorino, L. F. S. Alves, R. Wang, et al, "Low-Frequency Power Decoupling in Single-Phase Applications: A Comprehensive Overview," *IEEE Transactions on Power Electronics*, vol. 32, no. 4, pp. 2892-2912.

[9] M. Wu, C. Roberts and S. Hillmansen, "Modelling of AC feeding systems of electric railways based on a uniform multi-conductor chain circuit topology," *IET Conference on Railway Traction Systems (RTS 2010)*, pp. 1-5,2010.

[10] H. Hu, H. Tao, F. Blaabjerg, et al, "Train–Network Interactions and Stability Evaluation in High-Speed Railways–Part I: Phenomena and Modeling," *IEEE Transactions on Power Electronics*, vol. 33, no. 6, pp. 4627-4642, June 2018.